Proceedings of 20th International Congress on Acoustics, ICA 2010

23-27 August 2010, Sydney, Australia

Use of CFD to calculate the dynamic resistive end correction for microperforated materials

J. Stuart Bolton and Nicholas Kim

Ray W. Herrick Laboratories, Purdue University, West Lafayette In, USA

ABSTRACT

The classical Maa theory for microperforated materials was initially formulated for constant diameter, cylindrical holes. Since then, a number of *ad hoc* corrections have been suggested to account for different hole shapes, in particular, rounding of the aperture. Here it is shown that the resistance and reactance of small apertures may be calculated using relatively simple CFD models in which a single hole is modeled. The fluid is assumed to be viscous but incompressible, and the geometry is assumed to be axisymmetric. It will be shown that this approach essentially reproduces the classical theory of Maa for circular, sharp-edged apertures. However, it will also be shown that the empirical correction to the resistive end correction, in particular, exhibits a clear dependence on frequency and geometrical parameters that is neglected in conventional microperforated material models.

INTRODUCTION

Microperforated materials are of current interest since they provide a useful alternative to fibrous materials in a number of noise control situations. Thus it is important to be able to calculate the acoustical properties of microperforated materials accurately. The best-known model for microperforated materials is that of Maa [1], which is based on a model of oscillatory, viscous flow in small tubes. The Maa model also features end corrections to account for inertial and resistive effects associated with flow converging into the holes. Those corrections have usually been based on *ad hoc* comparisons between measured and predicted results. In the present work, an alternative approach has been adopted. Here a simple computational fluid dynamics (CFD) model of oscillatory, viscous flow through a single hole has been developed, and has been used to calculate the specific acoustic impedance of a microperforated sheet. In particular, the emphasis has been placed on the real part of the specific acoustic impedance (here referred to as the dynamic flow resistance) since the energy dissipation produced by a microperforated panel is represented by that component of the impedance. It will be shown that the CFD results for the dynamic flow resistance are in general agreement with the predictions of existing models, particularly at high frequencies, but that they differ significantly at low frequencies. It is suggested that the latter discrepancy results from the neglect of a static, resistive end correction in conventional microperforated material models. Based on the CFD results, a revised dynamic resistive end correction is proposed here. Note finally, that only sharp-edged holes have been considered in the present work, but that the general approach can easily be extended to calculate the specific acoustic impedance of microperforated materials having arbitrary hole geometries.

REVIEW OF THEORY

The Maa [1] model can be separated into two parts, one being a linear component and the other being a non-linear component which becomes significant at high incident sound pressure levels. In this study, the focus is on the linear part, only. The linear component of the Maa model is derived from Rayleigh's [2] formulation for wave propagation in narrow tubes. Based on those equations, Crandall [3] modeled a perforated plate, and Maa further developed Crandall's model for the case of very small holes in which the oscillatory viscous boundary layer spans the hole. For a circular-hole model, the equation of the normal specific transfer impedance of a microperforated sheet (without end correction) according to this model is expressed as:

$$z = \frac{j\omega t}{\sigma c}\left[1 - \frac{2}{k\sqrt{-j}}\frac{J_1(k\sqrt{-j})}{J_0(k\sqrt{-j})}\right]^{-1} \quad (1)$$

where ω is the angular frequency, t is a length of the hole (usually the same as the thickness of the perforated sheet), c is the speed of sound, σ is the surface porosity of the sheet (i.e., the fraction of the surface area occupied by holes), k is the perforation constant defined by $k = d\sqrt{\omega\rho/4\eta}$, η is the dynamic viscosity, ρ is the air density, d is the hole diameter, and J_0 and J_1 are the Bessel functions of the first kind of zeroth and first order, respectively.

A resistive end correction was suggested by Ingard [4], to account for energy dissipation at the surface of the sheet as flow approaches the hole. Ingard called this effect a surface resistance, and the surface resistance on one side of the hole was defined as $R_s = \frac{1}{2}\sqrt{2\eta\rho\omega}$. In the microperforated panel formulation of Guo *et al*. [5], the end correction is added to the real part of the above expression as:

$$r = Re\left\{\frac{j\omega t}{\sigma c}\left[1 - \frac{2}{k\sqrt{-j}}\frac{J_1(k\sqrt{-j})}{J_0(k\sqrt{-j})}\right]^{-1}\right\} + \frac{\alpha 2R_s}{\sigma\rho c} \quad (2)$$

where r is the real part of the specific transfer impedance, R_s is the surface resistance, and α is a nominally frequency-independent factor which accounts for hole type. It was suggested by Guo *et al.*, based on a comparison with measurements, that α should be set to 4 when the hole is sharp-edged, and should be set to 2 when the hole has a rounded edge.

Maa also used the surface resistance for the end correction, but he did not include a factor to account for hole shape.

In the present work, it has been found that the value of α in the above formulation is not necessarily independent of frequency. The objective here is to introduce a numerical procedure to identify the value of α which makes Eq. (2) exact for a given hole geometry.

CFD MODEL OF AN ORIFICE

Geometry

To perform the CFD calculations, it was first necessary to create a discretized model of a single, sharp-edged hole, and a corresponding channel. The microperforated panel was modeled geometrically using the software Gambit. The models were classified into 3 groups: one was a group having different panel thicknesses; the second was a group having different hole diameters; and the last was a group having different surface porosities. The mesh interval was chosen to be 0.005 mm in order to ensure accurate results for the smallest hole considered. In addition, the model was made axisymmetric (i.e., two-dimensional) to make the calculation time relatively short. Figure 1 shows the basic perforated panel model. Note that in Fig. 1, the bottom of the figure represents the center-line of the axisymmetric model.

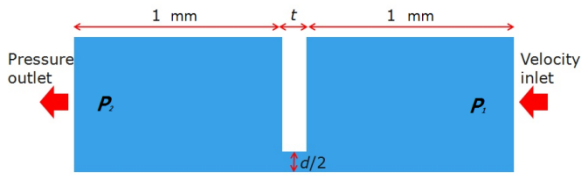

Figure 1. The geometry of the CFD model for a microperforated panel.

CFD parameters

The CFD calculations were performed by using the commercial software Fluent. Since all model dimensions were very small compared to a wavelength at all frequencies of interest, the flow was assumed to be incompressible, and as a result there was no energy loss by heat transfer. The simulation was a pressure-based, implicit formulation, the Green-Gauss node-based method was selected for the gradient option, and the second-order implicit method was chosen for the unsteady formulation. The options selected were: SIMPLE for the pressure-velocity coupling method, STANDARD for pressure, and SECOND-ORDER UPWIND for momentum. The outlet pressure was set to ambient pressure, and the inlet velocity was chosen to be a Hann windowed, 5 kHz half-sine wave having a maximum value of 1 mm/s in order to cover the frequency range up to 10 kHz. The simulations were run for 200 time steps over a period of 0.1 ms, and the time interval was 0.5 μs. The inlet velocity and the corresponding inlet pressure are shown in the Fig. 2(a), while the spectrum of the inlet velocity is shown in Fig. 2(b). Note that zero tangential velocity boundary conditions were imposed in the hole and on the surface of the plate section, but not at the outer surfaces of the inlet and outlet channel sections.

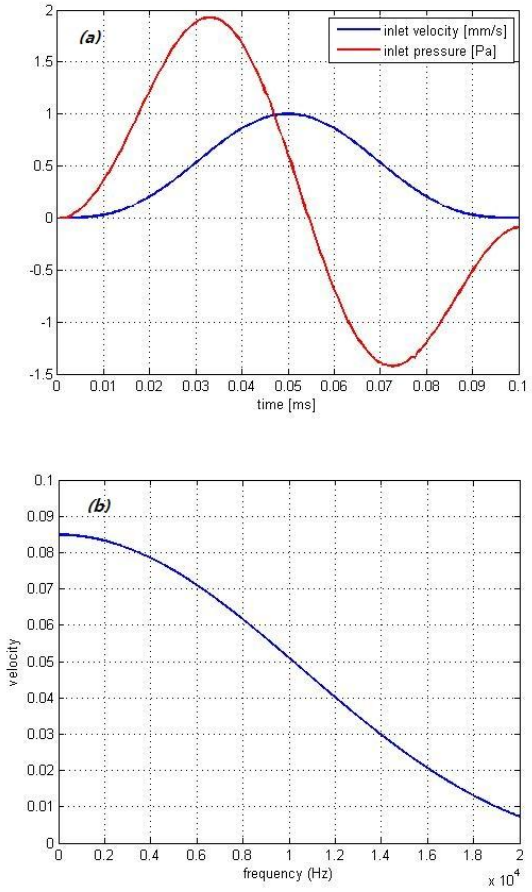

Figure 2. (a) Inlet velocity and pressure vs. time; **(b)** Inlet velocity magnitude vs. frequency.

As mentioned above, three sets of models were considered in which the following parameters were changed: panel thickness; hole diameter; and surface porosity. The specific parameters for three sets of models are listed in Table 1.

Table 1. Parameters of three model sets (t is thickness, d is diameter of the hole, σ is the surface porosity).

Set 1. Thickness			Set 2. Diameter			Set 3. Porosity		
t(mm)	d(mm)	σ	t(mm)	d(mm)	σ	t(mm)	d(mm)	σ
0.1016	0.4064	0.02	0.4064	0.1016	0.02	0.4064	0.2032	0.005
0.2032	0.4064	0.02	0.4064	0.2032	0.02	0.4064	0.2032	0.01
0.3048	0.4064	0.02	0.4064	0.3048	0.02	0.4064	0.2032	0.015
0.4064	0.4064	0.02	0.4064	0.4064	0.02	0.4064	0.2032	0.02
0.508	0.4064	0.02	0.4064	0.508	0.02	0.4064	0.2032	0.025
0.6096	0.4064	0.02	0.4064	0.6096	0.02	0.4064	0.2032	0.03
0.7112	0.4064	0.02				0.4064	0.2032	0.035
0.8128	0.4064	0.02				0.4064	0.2032	0.04
0.9144	0.4064	0.02						

Transfer impedance

The specific impedance of the panel was calculated as $Z = (P_1 - P_2)/V$. Here, P_1 is the inlet pressure, P_2 is the outlet pressure (which is the ambient pressure), and v is the inlet velocity; all of these quantities were Fourier transformed in order to obtain the impedance in the frequency-domain. The real part of the specific impedance is referred to here as the dynamic flow resistance, and the imaginary part is referred to as the dynamic flow reactance. Figure 3 shows the flow resistance and flow reactance for the three model sets described above.

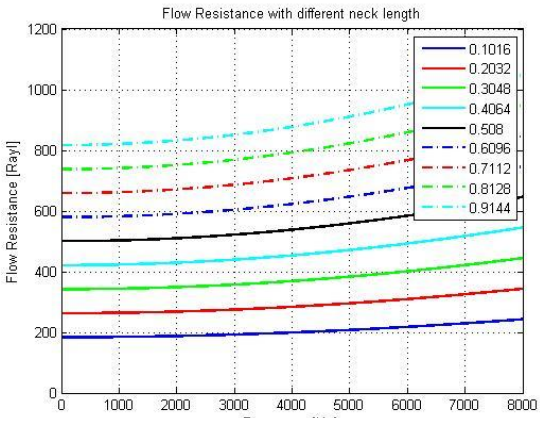

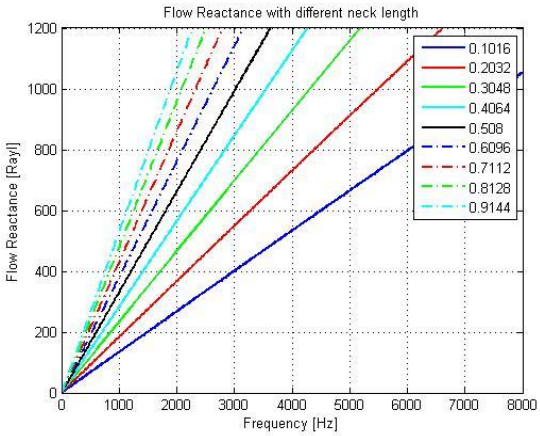

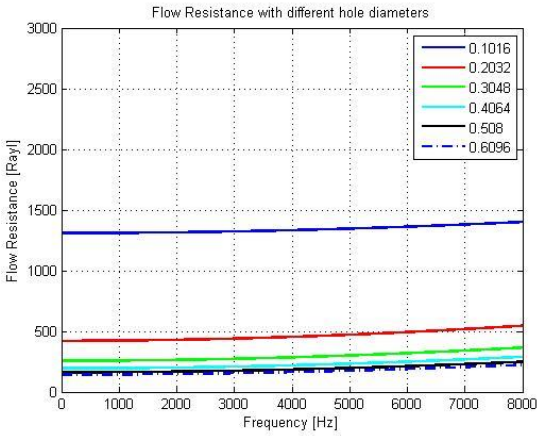

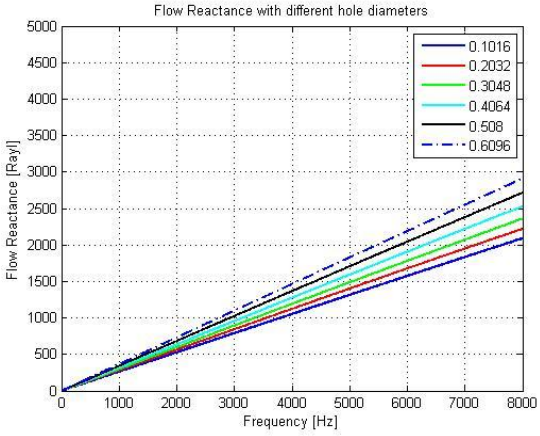

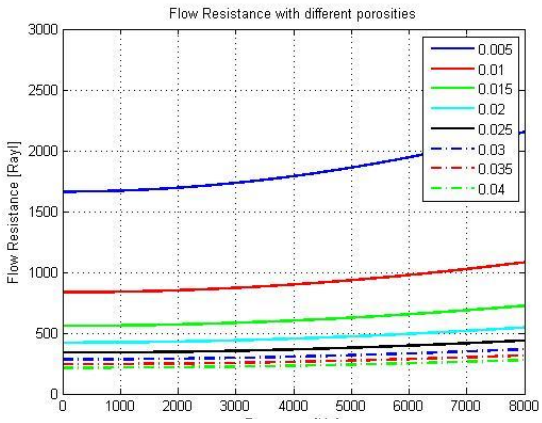

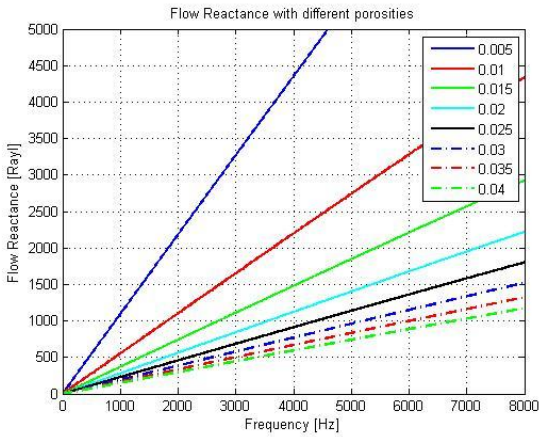

Figure 3. Dynamic flow resistance and dynamic flow reactance of set 1(top), set 2 (middle), and set 3 (bottom).

As expected, the dynamic flow resistance increases as the thickness increases, the diameter decreases, or the porosity decreases. The dynamic flow reactance, which will not be considered in detail here, shows a pure mass-like characteristic, as expected. To illustrate the difference between the CFD results and the predictions of the Guo et al. model, one particular case is considered here: the thickness of panel was 0.4064 mm, the hole diameter was 0.4064 mm, and the porosity was 0.02. In the Guo *et al*. model, the parameter α was set to 4, as suggested for a sharp-edged hole. The comparison of the impedances is shown in Fig. 4.

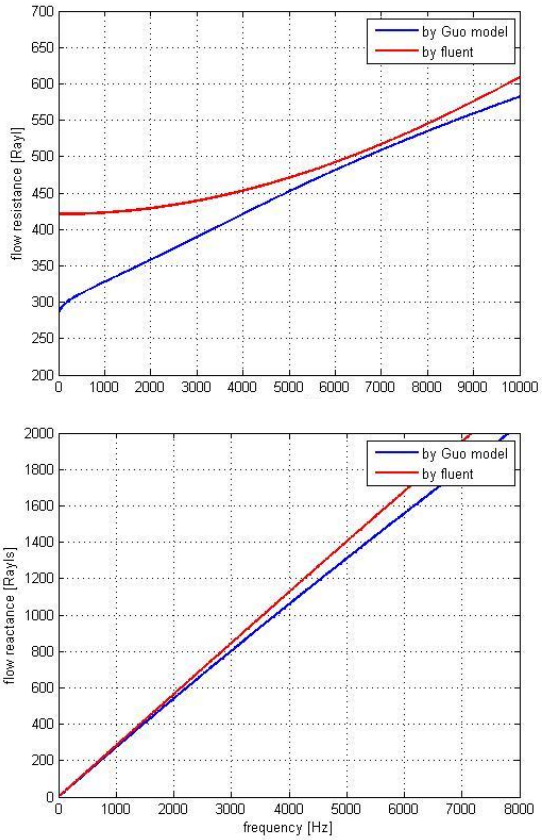

Figure 4. Dynamic flow resistance (above) and flow reactance (below) at d = 0.4064 mm, t = 0.4064 mm, σ = 0.02.

Both the dynamic flow resistance and reactance calculated from the CFD simulation are larger than predicted by the Guo *et al*. model, although the reactance is very similar in character. The two flow resistances are quite similar above 5 kHz, but differ in the low frequency range. It is suggested that the difference in the dynamic flow resistance at low frequencies results from the neglect of a static, resistive end correction in conventional microperforated material models. The resistive contribution to the hole impedance from flow over surfaces adjacent to the hole (and from shearing within the fluid exterior to the hole as flow converges into the hole) does not vanish at 0 Hz: i.e., under steady flow conditions. However, the assumed frequency dependence of the resistive end correction in the Guo *et al*. model (and in the Maa model on which it is based) necessarily causes the resistive end correction to become negligible at low frequencies (when the parameter α is assumed to be frequency-independent). This effect is believed to be primarily responsible for the difference between the Guo *et al*. and related models and the present CFD results, and this is the major finding of the current work.

DYNAMIC RESISTIVE END CORRECTION

As noted above, the main reason for the difference between the Guo *et al*. model and the CFD simulations results from the resistive end correction. The end correction in the Guo *et al*. model is expressed as $\frac{\alpha 2R_s}{\sigma\rho c}$, where α equals 4 for a sharp-edged hole. To improve the accuracy of the Guo et al. model, it would be necessary to make the parameter α dependent on frequency (as well as on the hole geometry and surface porosity). Here, the value of α has been calculated that would be required to force perfect agreement between the Guo *et al*. model (for the specific resistance) and the CFD results. Figure 5 shows the dependence of α on frequency and on geometric parameters, when defined in this way.

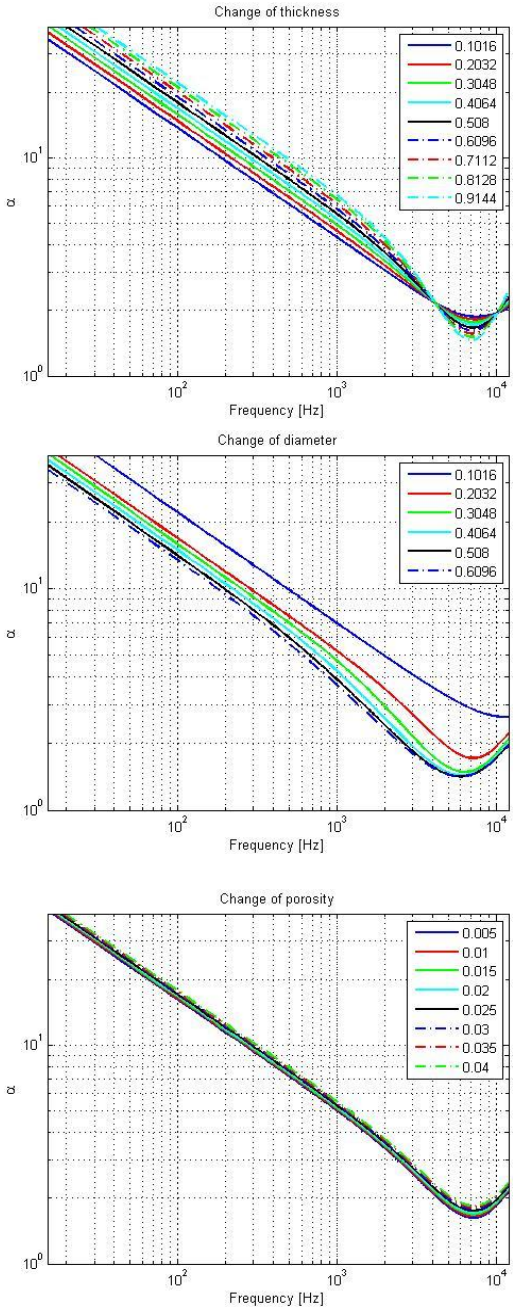

Figure 5. α vs. frequency for different thicknesses (left), different hole diameters (middle), and different surface porosities (right).

It can be seen that α is generally inversely proportional to frequency in the low frequency region, but that it appears to be approaching a constant value at high frequencies. The results in Fig. 5 also indicate that as the panel thickness increases, the value of α also increases. In the same way, the value of α increases as hole diameter decreases. In the variable porosity cases, the porosity does not have a strong effect in the range considered here, although it can be seen that α increases as porosity increases as expected (the resistive end correction would be expected to go to zero in the limit of surface porosity equal to unity). These results imply that α should, in principle, be treated as a function of frequency, thickness, hole diameter, and porosity. In the Fig. 5, all three

graphs show that α is approximately proportional to $f^{-0.5}$. Therefore, α can be conveniently represented as:

$$\propto = \beta f^{-0.5} \quad (3)$$

Then, a new parameter β, is defined to be a function of thickness, hole diameter, and porosity. Figure 6 shows β for different thicknesses, hole diameters, and porosities at 5 kHz.

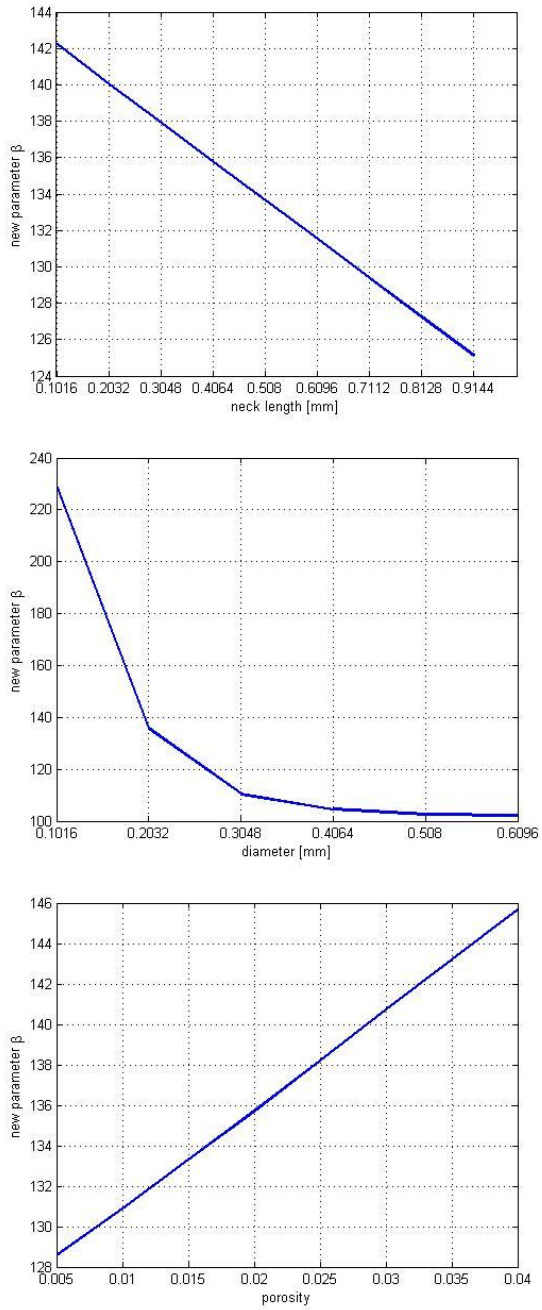

Figure 6. β vs. thickness (above), hole diameter (middle), and porosity (below) at 5000 Hz.

Figure 6 implies that β is proportional to porosity, and inversely proportional to thickness and hole diameter. Based on the change of flow resistance at 5 kHz, a new definition for the parameter β is suggested as :

$$\beta = (1.00 - 223t)\frac{\sigma}{d} + 135 \quad (4)$$

Eq. (3) shows that α depends on frequency, and Eq. (4) shows that α is function of thickness, hole diameter, and porosity. From these results, a new resistive end correction can be defined, based on Guo's end correction but in which the value of α is given as, $\propto = \beta f^{-0.5}$. Figures 7, 8, and 9 are comparisons of the value of α obtained by CFD simulation with that predicted using the new parameter β.

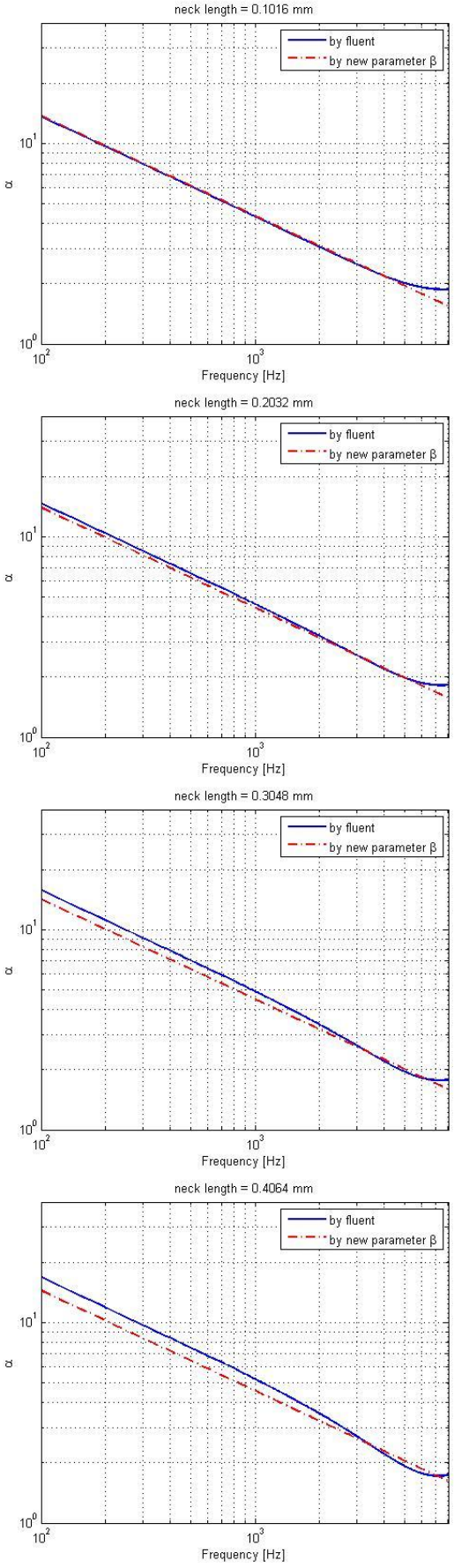

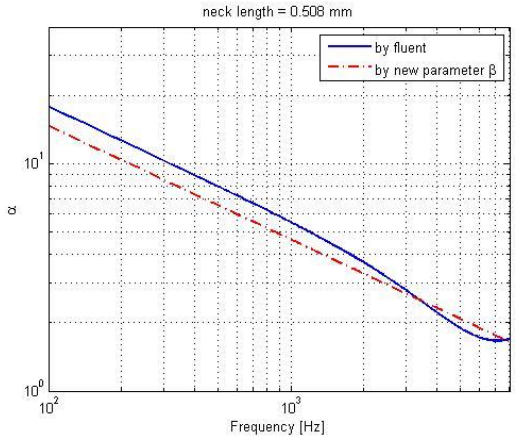

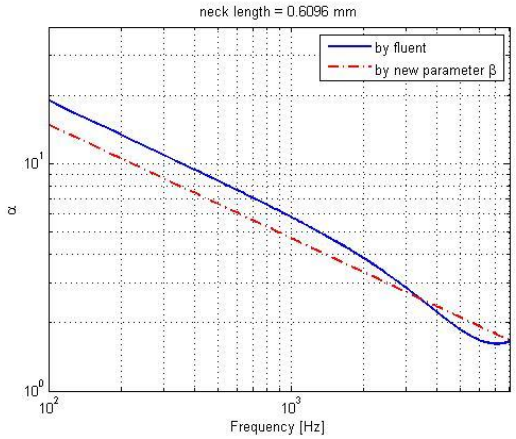

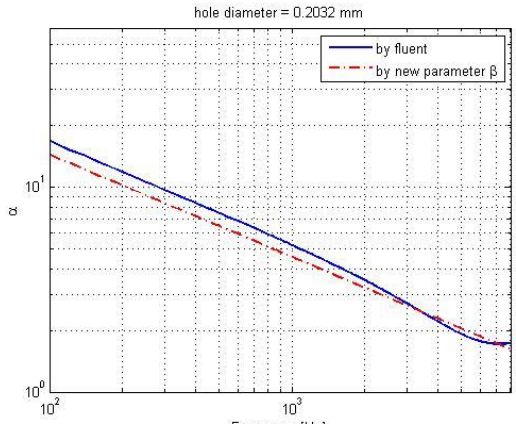

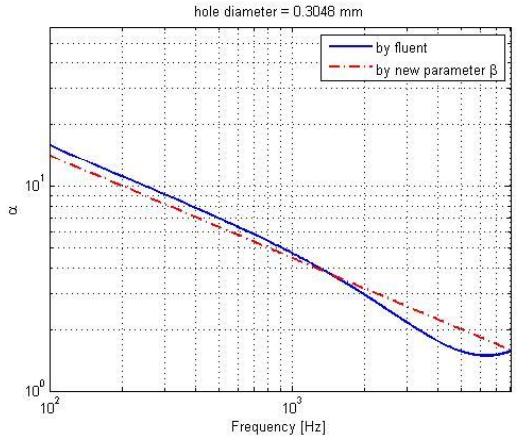

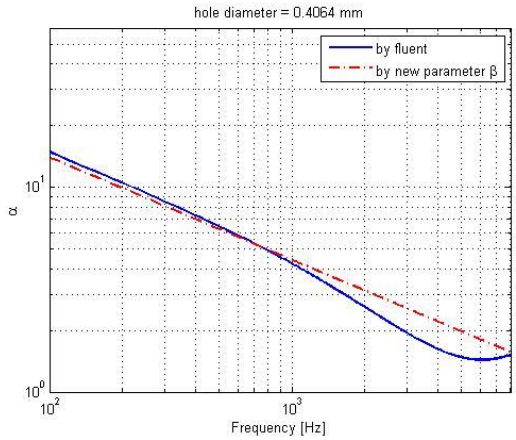

Figure 7. End correction from CFD simulation (blue line) vs. prediction with new parameter β (red line) at t = 0.1016, 0.2032, 0.3048, 0.4064, 0.508, 0.6096 mm (d = 0.2032 mm, σ = 0.02)

It can be seen from these results that the suggested form of the parameter β results in reasonable agreement between the CFD results and the approximate predictions over a relatively wide range of hole parameters.

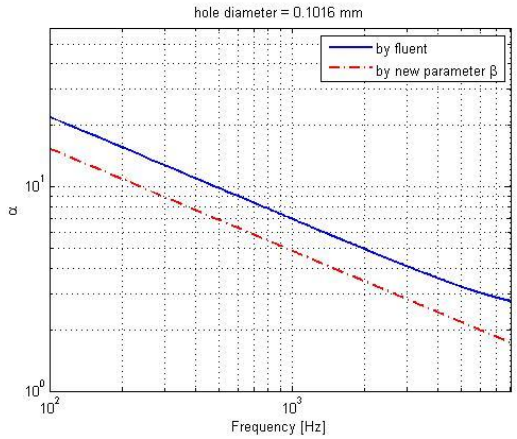

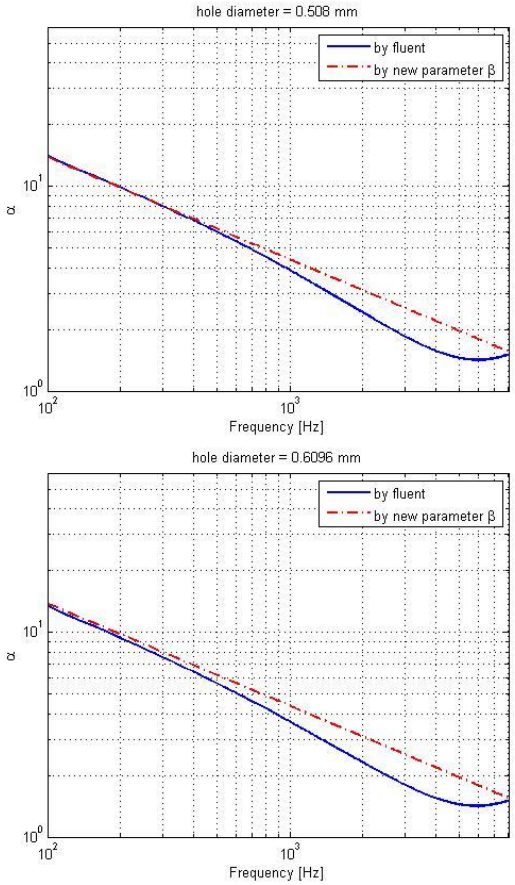

Figure 8. End correction from CFD simulation (blue line) vs. with new parameter β (red line) at d = 0.1016, 0.2032, 0.3048, 0.4064, 0.508, 0.6096 mm (t = 0.4064 mm, σ = 0.02)

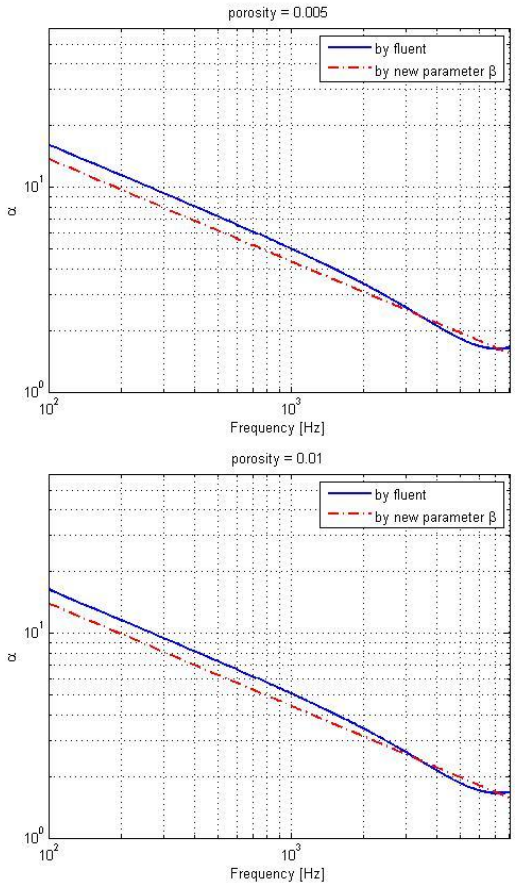

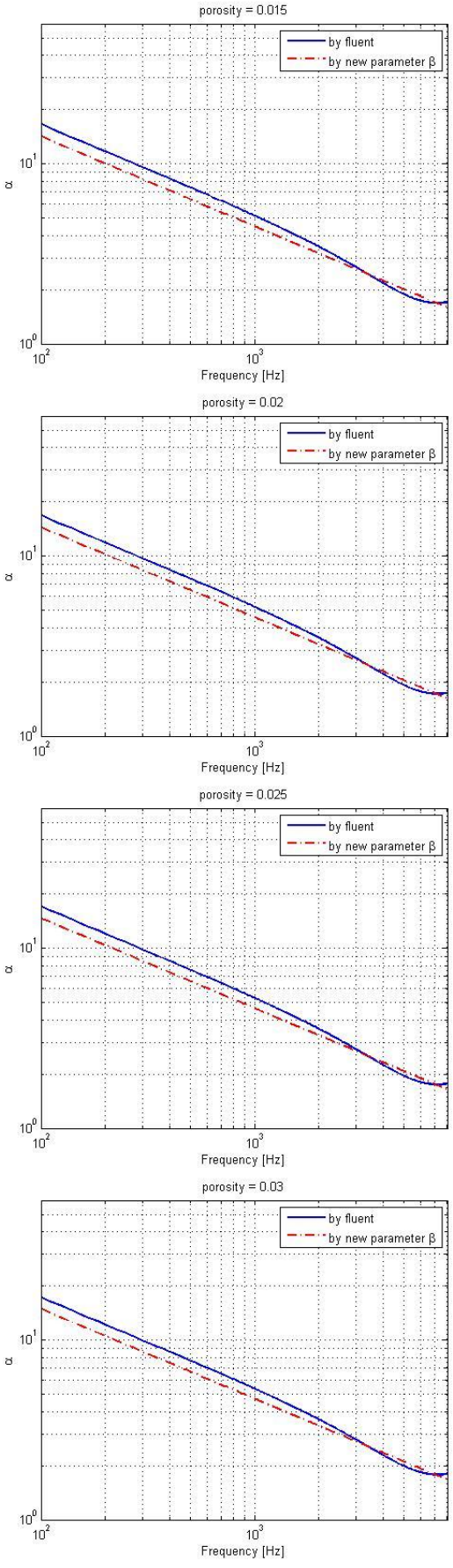

Figure 9. End correction from CFD simulation (blue line) vs. with new parameter β (red line) at σ = 0.005, 0.01, 0.015, 0.02, 0.025, 0.03 (d = 0.2032 mm, t = 0.2032 mm)

CONCLUSIONS

In this paper, CFD models of microperforated materials have been considered. It has been demonstrated that those models generally produce results that conform with well-established theoretical models, but may be more accurate at low frequencies, in particular. The CFD models have been used to generate corrections which can be applied to existing models to improve the accuracy of their predictions. Here, only square-edged holes have been considered, but the approach taken here can easily be extended to other hole geometries. An examination of the effect of varying hole geometry will be the subject of future work.

ACKNOWLEDGMENTS

The authors are grateful to Thomas Herdtle of 3M Corporation, St. Paul, Minnesota, for his useful, practical advice at an early stage of this work. The authors are also grateful to the National Aeronautics and Space Administration who supported this work through the Fundamental Aeronautics Subsonic Fixed Wing project under grant NNX07AV01A (monitor R.J. Silcox).

REFERENCES

1 D.Y. Maa. Theory and design of microperforated panel sound-absorbing constructions. Scientia Sinica, volume (18), 1975, 55-71.
2 Lord Rayleigh. Theory of Sound. McMillan, New York, 2nd edition, 1929.
3 I.B. Crandall. Theory of Vibrating Systems and Sound. Van Nostrand, New York, 2nd edition, 1926.
4 U. Ingard. On the theory and design of acoustics resonators. Journal of the Acoustical Society of America. Volume (25), 1953, 1037 - 1061
5 Y. Guo, S. Allam, and M. Abom. Micro-perforated plates for vehicle applications. INTER-NOISE 2008, Shanghai, China, 2008.